Mesoporous Films

DOI: 10.1002/ange.201108748

Highly Ordered Mesoporous Silica Films with Perpendicular Mesochannels by a Simple Stöber-Solution Growth Approach**

*Zhaogang Teng, Gengfeng Zheng, Yuqian Dou, Wei Li, Chung-Yuan Mou, Xuehua Zhang, Abdullah M. Asiri, and Dongyuan Zhao**

Surfactant-templated synthesis[1,2] has been a focus of materials science, because it provides a unique means to prepare a variety of ordered mesostructured materials with high surface areas and large, uniform pores. These materials have shown great promise for applications in physics, chemistry, and biology.[3–9] Different morphologies of mesoporous materials, such as spheres, films, monoliths, rods, and fibers, can all be controllably synthesized.[10,11] Among these, mesoporous thin films have attracted significant attention owing to their unique structures and functions.[12–15] Previously, ordered mesoporous silica films have been synthesized by self-assembly of silica precursors with surfactant templates at air–water[16] or water–oil interfaces,[17] or by using the evaporation-induced self-assembly (EISA) approach.[18] As the surfactant micelles tend to orient parallel to substrates to reduce the surface energy at interfaces, the mesochannels obtained are always oriented parallel to the film surfaces.[3,19–21] Continuous mesoporous films with perpendicularly aligned channels have recently been prepared by guiding the self-assembly of block copolymers or gemini surfactants with organosilica.[22–25] However, the thermal and mechanical stability of the films are low, as the pore walls consist of polymers and organosilica. Substrate-templating growth strategies for controlling mesopore orientation based on π–π or hydrophilic–hydrophobic interactions have been reported.[26–30] However, these methods require special substrates, such as pyrolytic graphite, anodic alumina with conical holes, or block polymer modified glass, and the alignment of the mesophases at their interface is generally of mixed orientation. Furthermore, perpendicular mesochannels have also been prepared by magnetic-field or electrochemically assisted methods.[31,32] However, these methods often require special equipment and complex processes, and the obtained films have poor regularity and low levels of mesochannel alignment. To date, the synthesis of films with mesopore channels perpendicular to a substrate is still a major challenge.

The Stöber approach is a facile and effective method for the synthesis of uniform mesoporous silica nanospheres by a self-assembly process using silica precursors with surfactant templates in an aqueous ethanol solution.[33] The ordered mesochannels in these mesoporous silica nanospheres are often oriented radially to the particle surfaces,[34–36] which is an ideal pore arrangement for applications such as catalysis and selective adsorption. Herein, we demonstrate a simple Stöber-solution growth method for the synthesis of mesoporous silica thin films with continuous 2D-ordered mesochannels perpendicular to the substrate. This is accomplished by immersing the substrate into a Stöber solution containing cetyltrimethylammonium bromide (CTAB), tetraethoxysilane (TEOS), ethanol, and ammonia. Moreover, a new type of sandwich-like mesoporous silica film, which tends to assemble into multilayer film arrays, has also been obtained.

The mesoporous silica films, both as-deposited and after removal of template, are transparent and retain the same size and shape as the substrates (Supporting Information, Figure S1 and S2), which are typically over several square centimeters in area and can be readily scaled up to any size. A top-view SEM image (Figure 1a) shows that the mesoporous silica films are continuous over a large domain without cracking. They are quite stable: even after being calcined at 500 °C, no cracks are formed. Employing a typical ethanol/water ratio of 0.43 and an ammonia concentration of 1.4 mM at 60 °C over 3 days, resulted in a highly uniform mesoporous silica film, with a thickness of about 155 nm and variation of less than 3% (Figure 1b). A cross-section TEM image (Figure 1c) of the thin film directly after detachment from the glass substrate shows a smooth surface and a uniform thickness of about 155 nm, implying a good mechanical stability. The mesochannels, fully oriented perpendicular to

[*] Dr. Z. Teng, Prof. G. Zheng, Dr. Y. Dou, W. Li, Prof. D. Y. Zhao
Department of Chemistry, Shanghai Key Laboratory of Molecular Catalysis and Innovative Materials, Laboratory of Advanced Materials, Fudan University
Shanghai 200433, (P.R. China)
E-mail: dyzhao@fudan.edu.cn
Prof. Dr. C.-Y. Mou
Department of Chemistry, National Taiwan University (Taiwan)
Dr. X. Zhang
Department of Chemical and Biomolecular Engineering, University of Melbourne (Australia)
and
Faculty of Life and Social Sciences, Swinburne University of Technology (Australia)
Prof. A. M. Asiri
Chemistry Department and the Center of Excellence for Advanced Materials Research, King Abdul-Aziz University (Saudi Arabia)

[**] This work was supported by the NSF of China (20890123), the State Key Basic Research Program of the PRC (2009AA033701 and 2009CB930400), the Science and Technology Commission of Shanghai Municipality (08DZ2270500), and the Shanghai Leading Academic Discipline Project (B108). Z.T. thanks the National Science Foundation for Post-doctoral Scientists of China (20100480030) and the Shanghai Postdoctoral Sustentation Fund (11R21411500) for financial support. We thank the Instrument Center of Central University in Taiwan for measuring the GISAX data.

Supporting information for this article is available on the WWW under http://dx.doi.org/10.1002/anie.201108748.

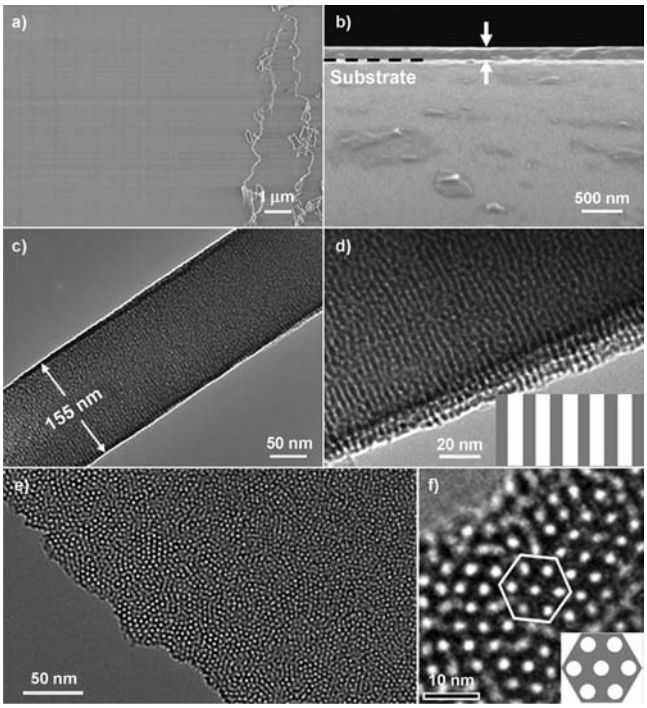

Figure 1. Images of the mesoporous silica films deposited on glass by the Stöber-solution spontaneous growth method. a) Top-view SEM image of the film. b) Cross-section SEM image of a film deposited on glass after vertical cleaving. c, d) Cross-section TEM images. e, f) Top-view TEM images. Insets in (d) and (f) are the structural models of the cross-section and surface of the mesoporous silica film, respectively.

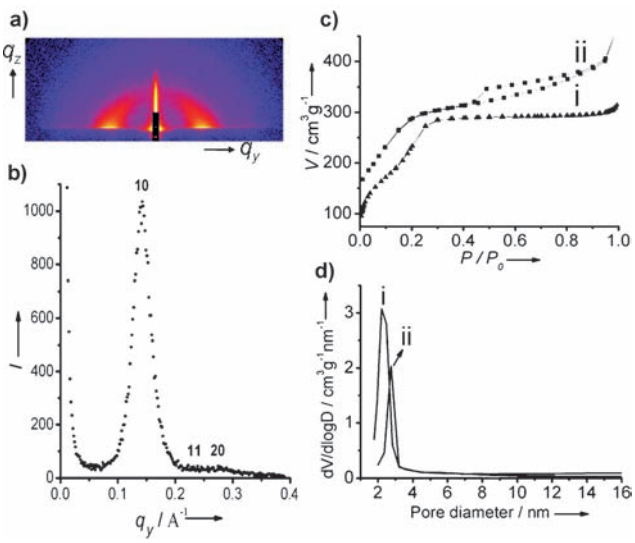

Figure 2. a) 2D-GISAXS scattering profiles of the mesoporous silica films prepared by the Stöber-solution spontaneous growth method. b) Intensity profiles plotted against q_y for the GISAXS patterns shown in (a). c) Nitrogen sorption isotherms and (d) Pore size distribution curves of the mesoporous silica films grown at i) 60 °C and ii) 100 °C.

the substrate, are continuous throughout a cross-section of the film and possess openings at both ends (Figure 1 d). Top-view TEM images (Figure 1 e,f) reveal an ordered, hexagonal packing of mesopores over the entire film without any mesochannel strips, suggesting that all the mesopore channels are perpendicular to the surface. The average center-to-center distance between two adjacent mesochannels is about 4.1 nm, and the pore size is roughly estimated at 2.3 nm.

The perpendicular mesochannels over the entire film have been further characterized by XRD (Supporting Information, Figure S3). No out-of-plane XRD reflection is observed in the thin film obtained, suggesting that no mesostructures are oriented parallel to the substrate. The 2D grazing-incidence small-angle X-ray scattering (GISAXS) pattern of the mesoporous silica film (Figure 2 a) shows two prominent spots on the left and right of the grazing incidence X-ray beam that correspond to the scattering wave vectors parallel to the surface of the film, indicating that the mesochannels are oriented perpendicular to the surface.[37,38] The 1D intensity profiles of the mesoporous silica film collected in each case are plotted against q_y of the GISAXS data (Figure 2 b). The peak positions in the mesoporous silica films correspond to a d spacing of 4.3 nm, which is in agreement with the TEM results. The small-angle X-ray scattering pattern of the mesoporous silica film shows three diffraction peaks, associated with the 10, 11, and 20 reflections of hexagonal symmetry with the space group *p6mm*. This is in good agreement with that of the as-made bulk mesoporous silica MCM-41 (Mobil crystalline material),[1,2] suggesting a similar ordered hexagonal mesostructure.

Nitrogen adsorption–desorption isotherms of the mesoporous silica film grown at 60 °C shows a characteristic type IV curve (Figure 2 c, curve i), indicating a uniform mesopore architecture. No hysteresis loop is observed, similar to that of small-pore MCM-41. The surface area and pore volume are calculated to be as high as about 834 $m^2 g^{-1}$ and 0.49 $cm^3 g^{-1}$, respectively. Moreover, the film has a pore size of about 2.3 nm with a narrow distribution (Figure 2 d, curve i), a value consistent with that obtained by TEM and indicative of uniform mesopores in the film.

The entire silica film can be easily detached from the growth substrate to form a free-standing structure when indium tin oxide (ITO) glass is used as a substrate (Supporting Information, Figure S2), which is accomplished by etching the substrate in a concentrated (8 M) HNO_3 solution at room temperature after the desired film growth has been achieved. The large domain size and intact morphology of the resulting free-standing mesoporous silica films are indicative of their high mechanical and chemical stability, which can facilitate potential applications as nanodevices on different substrates.

To investigate the growth process of the mesoporous silica films, they were synthesized by tuning different reaction parameters, including ethanol/water ratio, ammonia concentration, CTAB/TEOS ratio, growth time, and reaction temperature. It was found that ethanol plays an important role in film growth. The film thickness can be varied from 34 to 110 nm by adjusting ethanol/water ratio from 0.2 to 0.53 (Supporting Information, Figure S4a). When the ethanol/water ratio is higher than 1.0, the structural ordering of the mesoporous silica films is disrupted. On the other hand, reducing the ratio to less than 0.2 yields disordered mesopores in the silica films (Figure S5) and numerous uniform mesoporous silica spheres with a diameter of about 50 nm (Fig-

ure S6). However, highly ordered mesochannels and hexagonal mesostructures are observed in all domains across these silica spheres (Figure S6 and S7). The ammonia concentration is another important factor for film growth. Increasing it to greater than 14 mM leads to a significant decrease in film thickness, while simultaneously yielding large quantities of mesoporous silica spheres as by-products. This is most likely due to an increase in the TEOS hydrolysis and condensation rates owing to the higher ammonia concentration, which is a competitive process with film growth, thus resulting in a decrease in film thickness (Figure S4b). With an increase in the CTAB/TEOS ratio, the thickness of the mesoporous silica films increases from 90 to 155 and then to 240 nm (Figure S4c). In addition, by depositing the substrates in the Stöber solution for 1, 2, or 3 days, an increase in the film thickness to 48, 95, or 155 nm, respectively, was observed. This is suggestive of a time-dependent growth process (Figure S4d). The film growth rate was calculated to be about 2 nm h^{-1}.

Moreover, when the growth temperature was increased to 100 °C, a new type of sandwich-like mesoporous silica film with three layers of mesostructures and a uniform thickness of 75 nm was discovered (Figure 3a). Cross-section TEM images show that the mesoporous silica films also possess perpendicular mesochannels with a periodic spacing of about 4.0 nm. Top views of the mesoporous silica films show that the ordered mesopores are present throughout the entire domain, although some defects in the mesopore channels with spacings of 10–40 nm are present inside the film (Figure 3b). These correspond to the middle layers observed in the cross-section TEM images in Figure 3a. The detached sandwich-like mesoporous silica thin films tend to pack against each other in water and form self-assembled multilayer film arrays (Figure 3c). The nitrogen sorption isotherm of the sandwich-like mesoporous silica films (Figure 2c, curve ii) also shows a typical type IV curve with a distinct hysteresis loop of H2 in the p/p_0 range of 0.4–1.0, implying that ink-bottle-like mesopores resulted from the defects. The surface area and the pore volume are as high as 1011 $m^2 g^{-1}$ and 0.72 $cm^3 g^{-1}$, respectively, and the pore size is uniform, namely about 2.8 nm (Figure 2d, curve ii).

Based on the above results, we propose that the growth process of these mesoporous silica films, with perpendicular mesochannels (Figure 4), proceeds through a gradual transformation of silicate–CTAB composites from spherical to

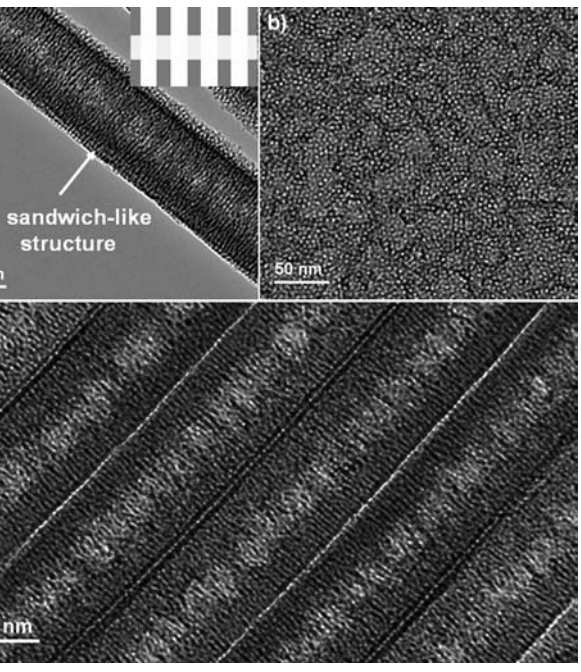

Figure 3. TEM images of sandwich-like mesoporous silica films. a) Cross-section view. b) Top view. c) Cross-sectional view of self-assembly arrays for the silica films. Inset in (a) is the structural model for the sandwich-like structure.

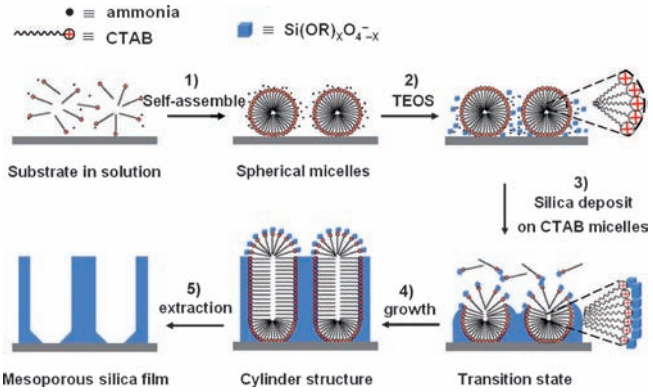

Figure 4. Illustration of the formation process of ordered mesoporous silica films with perpendicular mesochannels by the Stöber-solution spontaneous growth procedure.

cylindrical micelles with the assistance of ammonia hydrogen bonding and controlled silicate polymerization. In a Stöber solution, the surfactant cations (CTA^+) are first strongly adsorbed on a negatively charged substrate (such as glass or ITO), and form spherical CTAB micelle assemblies on the substrate surface (step 1),[39] as opposed to the rod-shaped micelles formed by other polymeric surfactants that are commonly laid on substrates to reduce surface energy and subsequently induce mesochannels parallel to substrate surface.[40] When TEOS molecules are added, they are slowly hydrolyzed in an ammonia and ethanol solution with controlled concentration to form negatively charged oligomeric silicate species which approach the spherical micelle surface through electrostatic interaction (step 2). At low concentrations, these free silicate species are preferentially deposited at the junction between the spherical micelles and the substrate, which is expected to screen the intra-micelle electrostatic repulsion among adjacent head groups.[41] Simultaneously, the diffusion of ethanol into the CTAB micelles reduces the interaction of the alkyl tails, which increases the hydrophobic volume of the micelles and lowers their curvature.[42,43] Furthermore, the presence of ammonia facilitates the formation hydrogen bonds between the adjacent CTAB micelles and silicate oligomers, which also favors the formation of parallel mesochannels to reduce the curvature energy of the micelles. Owing to these three factors, the CTAB–silicate composites undergo a structure transition from spherical to

cylindrical micelles (step 3). With the continuous diffusion and re-assembly of CTAB molecules, newly hydrolyzed silicate oligomers are adsorbed and cross-linked onto the charged micelle head groups at the solution–silica film interface, leading to a continuous, large-domain film growth along with the longitudinal direction of cylindrical micelles that are perpendicularly orientated on the substrate (step 4). Previously reported Monte Carlo simulation results also showed that a highly active interface induces a perpendicular alignment in surfactant mesophases.[44] After solution assembly and growth, mesoporous silica films with perpendicular channels are subsequently obtained through the removal of surfactants by solvent extraction (step 5). The silica mesostructure may undergo a reorganization process from a disordered to an ordered structure. The interface nucleation and slow growth, which are kinetically controlled in the Stöber solution, play an important role in the formation of the perpendicular mesochannels.

Along with our newly demonstrated film growth on substrates, the growth of mesoporous silica spheres in the Stöber solution is a competitive growth route, as has been recently reported.[36] An increase in the ammonia concentration can enhance the hydrolysis and condensation rates for TEOS to form substantial silicate oligomers, which are assembled with CTAB molecules and form mesoporous silica spheres in the solution, resulting in a decrease in film thickness on the substrate. Similarly, the hydrolysis and condensation rates of silicates can be significantly increased by decreasing the ethanol/water ratio, leading to more silica particles formed in the solution and a decrease in the silica film thickness. Moreover, when the reaction temperature is increased to 100 °C,[45] the silica films formed can be slowly redissolved, and the interfaces between the substrate and solution migrate outward until an equilibrium is reached.[46,47] This process results in the reorganization of the mesostructure and formation of hollow structures in the new sandwich-like mesoporous silica films, as with the "rattle" nanoparticles previously observed.[46]

In summary, we report the first successful synthesis of large, uniform mesoporous silica thin films with ordered perpendicular mesopore channels by a Stöber-solution spontaneous growth approach. The key to the formation of continuous mesoporous silica films is the controlled gradual transition of CTAB–silicate composites from spherical to cylindrical micelles through ammonia-catalyzed self-oriented growth at the solution–substrate interface. The mesochannels of the obtained mesoporous silica films are highly oriented and perpendicular to the substrate, with excellent mechanical and chemical properties. Also, a new type of sandwich-like mesoporous silica film with many mesochannel defects has been synthesized by the Stöber-solution growth method at a high reaction temperature. As this method can be generally applied to different materials and morphologies, a variety of highly ordered 2D architectures and free-standing films with perpendicular mesochannels can be realized, providing many new and exciting opportunities in the fabrication of functional devices for optics, electronics, electrochemistry, biomolecule separation, and so on.

Received: December 12, 2011
Published online: January 24, 2012

Keywords: mesoporous materials · perpendicular channels · silica · Stöber solution · thin films

[1] C. T. Kresge, M. E. Leonowicz, W. J. Roth, J. C. Vartuli, J. S. Beck, *Nature* **1992**, *359*, 710 – 712.
[2] J. S. Beck, J. C. Vartuli, W. J. Roth, M. E. Leonowicz, C. T. Kresge, K. D. Schmitt, C. T.-W. Chu, D. H. Olson, E. W. Sheppard, S. B. McCullen, J. B. Higgins, J. L. Schlenker, *J. Am. Chem. Soc.* **1992**, *114*, 10834 – 10844.
[3] H. Yang, A. Kuperman, N. Coombs, S. Mamiche-Afara, G. A. Ozin, *Nature* **1996**, *379*, 703 – 705.
[4] D. Feng, Y. Lv, Z. Wu, Y. Dou, L. Han, Z. Sun, Y. Xia, G. Zheng, D. Zhao, *J. Am. Chem. Soc.* **2011**, *133*, 15148 – 15156.
[5] Z. Teng, J. Li, F. Yan, R. Zhao, W. Yang, *J. Mater. Chem.* **2009**, *19*, 1811 – 1815.
[6] J. S. Lee, X. Wang, H. Luo, G. A. Baker, S. Dai, *J. Am. Chem. Soc.* **2009**, *131*, 4596 – 4597.
[7] M. Xu, D. Feng, R. Dai, H. Wu, D. Zhao, G. Zheng, *Nanoscale* **2011**, *3*, 3329 – 3333.
[8] B. J. Melde, B. J. Johnson, D. T. Charles, *Sensors* **2008**, *8*, 5202 – 5228.
[9] Q. Huo, D. Zhao, J. Feng, K. Weston, S. K. Buratto, G. D. Stucky, S. Schacht, F. Schuth, *Adv. Mater.* **1997**, *9*, 974 – 978.
[10] J. Li, J. Liu, D. Wang, R. Guo, X. Li, W. Qi, *Langmuir* **2010**, *26*, 12267 – 12272.
[11] M. Steinhart, C. Liang, G. W. Lynn, U. Gösele, S. Dai, *Chem. Mater.* **2007**, *19*, 2383 – 2385.
[12] H. Yang, N. Coombs, G. A. Ozin, *Nature* **1997**, *386*, 692 – 695.
[13] J. W. Park, S. S. Park, Y. Kim, I. Kim, C. S. Ha, *ACS Nano* **2008**, *2*, 1137 – 1142.
[14] C. H. Hou, X. Wang, C. Liang, S. Yiacoumi, C. Tsouris, S. Dai, *J. Phys. Chem. B* **2008**, *112*, 8563 – 8570.
[15] S. S. Park, Y. Jung, C. Xue, R. Che, D. Zhao, C. S. Ha, *Chem. Mater.* **2010**, *22*, 18 – 26.
[16] H. Yang, N. Coombs, I. Sokolov, G. A. Ozin, *Nature* **1996**, *381*, 589 – 592.
[17] S. Schacht, Q. Huo, I. G. Voigt-Martin, G. D. Stucky, F. Schuth, *Science* **1996**, *273*, 768 – 771.
[18] Y. Lu, R. Ganguli, C. A. Drewien, M. T. Anderson, C. J. Brinker, W. Gong, Y. Guo, H. Soyez, B. Dunn, M. H. Huang, J. I. Zink, *Nature* **1997**, *389*, 364 – 368.
[19] L. Nicole, C. Boissiere, D. Grosso, A. Quach, C. Sanchez, *J. Mater. Chem.* **2005**, *15*, 3598 – 3627.
[20] H. Miyata, W. Kubo, A. Sakai, Y. Ishida, T. Noma, M. Watanabe, A. Bendavid, P. J. Martin, *J. Am. Chem. Soc.* **2010**, *132*, 9414 – 9419.
[21] J. Otomo, S. Wang, H. Takahashi, H. Nagamoto, *J. Membr. Sci.* **2006**, *279*, 256 – 265.
[22] A. Chen, M. Komura, K. Kamata, T. Iyoda, *Adv. Mater.* **2008**, *20*, 763 – 767.
[23] H. Fukumoto, S. Nagano, N. Kawatsuki, T. Seki, *Chem. Mater.* **2006**, *18*, 1226 – 1234.
[24] C. Ma, L. Han, Z. Jiang, Z. Huang, J. Feng, Y. Yao, S. Che, *Chem. Mater.* **2011**, *23*, 3583 – 3586.
[25] S. Park, D. H. Lee, J. Xu, B. Kim, S. W. Hong, U. Jeong, T. Xu, T. P. Russe, *Science* **2009**, *323*, 1030 – 1033.
[26] M. Hara, S. Nagano, T. Seki, *J. Am. Chem. Soc.* **2010**, *132*, 13654 – 13656.
[27] V. R. Koganti, D. Dunphy, V. Gowrishankar, M. D. McGehee, X. F. Li, J. Wang, S. E. Rankin, *Nano Lett.* **2006**, *6*, 2567 – 2570.
[28] Y. Yamauchi, T. Nagaura, A. Ishikawa, T. Chikyow, S. Inoue, *J. Am. Chem. Soc.* **2008**, *130*, 10165 – 10170.

[29] E. K. Richman, T. Brezesinski, S. H. Tolbert, *Nat. Mater.* **2008**, *7*, 712 – 717.
[30] K. C. W. Wu, X. Jiang, Y. Yamauchi, *J. Mater. Chem.* **2011**, *21*, 8934 – 8939.
[31] Y. Yamauchi, M. Sawada, T. Noma, H. Ito, S. Furumi, Y. Sakka, K. Kuroda, *J. Mater. Chem.* **2005**, *15*, 1137 – 1140.
[32] A. Walcarius, E. Sibottier, M. Etienne, J. Ghanbaja, *Nat. Mater.* **2007**, *6*, 602 – 608.
[33] M. Grün, I. Lauer, K. K. Unger, *Adv. Mater.* **1997**, *9*, 254 – 257.
[34] R. I. Nooney, D. Thirunavukkarasu, Y. Chen, R. Josephs, A. E. Ostafin, *Chem. Mater.* **2002**, *14*, 4721 – 4728.
[35] Z. Teng, Y. Han, J. Li, F. Yan, W. Yang, *Microporous Mesoporous Mater.* **2010**, *127*, 67 – 72.
[36] Y. H. Deng, D. Qi, C. H. Deng, X. M. Zhang, D. Y. Zhao, *J. Am. Chem. Soc.* **2008**, *130*, 28 – 29.
[37] D. M. Smilgies, P. Busch, D. Posselt, C. M. Papadakis, *Synchrotron Radiat. News* **2002**, *15*, 35 – 42.
[38] S. H. Kim, M. J. Misner, T. P. Russell, *Adv. Mater.* **2004**, *16*, 2119 – 2123.
[39] S. Manne, H. E. Gaub, *Science* **1995**, *270*, 1480 – 1482.
[40] P. C. A. Alberius, K. L. Frindell, R. C. Hayward, E. J. Kramer, G. D. Stucky, B. F. Chmelka, *Chem. Mater.* **2002**, *14*, 3284 – 3294.
[41] A. Firouzi, D. Kumar, L. M. Bull, T. Besier, P. Sieger, Q. Huo, S. A. Walker, J. A. Zasadzinski, C. Glinka, J. Nicol, D. Margolese, G. D. Stucky, B. F. Chmelka, *Science* **1995**, *267*, 1138 – 1143.
[42] X. Auvray, T. Perche, C. Petipas, R. Anthore, M. J. Marti, I. Rico, A. Lattes, *Langmuir* **1992**, *8*, 2671 – 2679.
[43] M. T. Anderson, J. E. Martin, J. G. Odinek, P. P. Newcomer, *Chem. Mater.* **1998**, *10*, 311 – 321.
[44] S. E. Rankin, A. P. Malanoski, F. van Swol, *Mater. Res. Soc. Symp. Proc.* **2001**, *636*, 121 – 126.
[45] G. B. Alexander, W. M. Heston, R. K. Iler, *J. Phys. Chem.* **1954**, *58*, 453 – 455.
[46] Q. Yu, P. Wang, S. Hu, J. Hui, J. Zhuang, X. Wang, *Langmuir* **2011**, *27*, 7185 – 7191.
[47] T. Zhang, J. Ge, Y. Hu, Q. Zhang, S. Aloni, Y. Yin, *Angew. Chem.* **2008**, *120*, 5890 – 5895; *Angew. Chem. Int. Ed.* **2008**, *47*, 5806 – 5811.

